Heliyon 10 (2024) e37882

Contents lists available at ScienceDirect

Heliyon

journal homepage: www.cell.com/heliyon

Research article

Investigation of biochars derived from waste lignocellulosic biomass and insulation electric cables: A comprehensive TGA and Macro-TGA analysis

Roberta Panizio [a,b], Carlos Castro [c], Nuno Pacheco [c], Ana Carolina Assis [a], Andrei Longo [a], Cândida Vilarinho [c], José Carlos Teixeira [c], Paulo Brito [a], Margarida Gonçalves [a,b], Catarina Nobre [a,*]

[a] VALORIZA, Research Center for Endogenous Resource Valorization, Portalegre Polytechnic University, 7300- 555, Portalegre, Portugal
[b] MEtRICs, Mechanical Engineering and Resource Sustainability Center, Chemistry Department, SST-NOVA University of Lisbon, 2829-516, Caparica, Portugal
[c] MEtRICs, Mechanical Engineering and Resource Sustainability Center, Mechanical Engineering Department, School of Engineering, University of Minho, 4804-533, Guimarães, Portugal

ARTICLE INFO

Keywords:
Waste valorization
Biochar
Macro-TGA
Polymeric waste
E-Waste

ABSTRACT

This study investigates the thermochemical decomposition and gasification performance of biochars produced from blends of waste lignocellulosic biomass and waste insulation electrical cables at varying temperatures. Characterization tests revealed changes, particularly in ash content (27.5 %–34 %) and elemental composition, with nitrogen content increasing notably in biochar samples compared to the original feedstock. Van Krevelen diagrams demonstrated a reduction in O/C and H/C ratios with increasing production temperature, resembling fossil fuels more closely. The thermogravimetric and the derived thermogravimetric profiles illustrated distinct degradation stages influenced by heating rates and production temperature. Macro-TGA tests provided insights into biomass residue behavior under gasification conditions, indicating higher reaction rates at elevated temperatures. Syngas analysis highlighted the impact of temperature and equivalence ratio on syngas composition, with higher temperatures favoring hydrogen-rich gas production. The observed trends in cold gas efficiency (42.61 %–50.40 %) and carbon conversion efficiency (45.83 %–50.40 %) underscore the significance of temperature control in maximizing gasification performance. Biochars produced at higher temperatures demonstrated superior gasification performance, suggesting potential for optimizing biochar production processes to enhance energy recovery and waste valorization.

1. Introduction

Waste from electrical and electronic equipment (WEEE) is the fastest-growing waste stream and is becoming a major environmental problem, mainly for developing and emerging economies [1–4]. The increased WEEE amounts make it difficult for recycling to keep up with this growth, with global amounts rising by more than 9.0 Mt, producing a total amount of 53.9 Mt in 2019 distributed in Africa

* Corresponding author.
E-mail address: catarina.nobre@ipportalegre.pt (C. Nobre).

https://doi.org/10.1016/j.heliyon.2024.e37882
Received 31 May 2024; Received in revised form 9 August 2024; Accepted 11 September 2024
Available online 12 September 2024

Nomenclature and abbreviations

Al	Aluminium
B300	Biochar 300 °C
B350	Biochar 350 °C
B400	Biochar 400 °C
BFRs	Brominated flame retardants
Br	Bromine
C	Carbon
CO	Carbon monoxide
CO_2	Carbon dioxide
Di	Ignition index
EU	European Union
H_2	Hydrogen
H_2O	Water
HCl	Hydrochloric acid
Mt	mega tonne
Ni	Nickel
O	Oxygen
PE	Polyethylene
PP	Polypropylene
PS	Polystyrene
PVC	Polyvinyl chloride
TGA	Thermogravimetric analysis
WEEE	Waste from electrical and electronic equipment
WIEC	Waste insulation electric cables
WLB	waste lignocellulosic biomass
ZSM-5	Zeolite Socony Mobil–5

(2.9 Mt), America (13.1 Mt), Asia (24.9 Mt), Europe (12 Mt) and Oceania (0.7 Mt) [1,5]. Increasing consumption, associated with the short useful life and limited repair options of certain technologies, are the main reasons for the increase in WEEE generation rates [6,7]. In the European Union (EU), WEEE production presents annual growth rates of 2 %. Estimates indicate that less than 40 % of these wastes are recycled. Nevertheless, Portugal contradicts this tendency since data for this country shows a recycling value of 43.5 % of electrical and electronic equipment in 2017 [8].

Plastics are present in different proportions in WEEE, particularly in waste insulation electric cables (WIEC). Varying according to size and characteristics, plastics can serve as housing, casing, insulation, internal shelves, or linings in electrical and electronic equipment. The amount of plastic in WEEE has been determined to range between 3.5 and 45 wt% [9,10]. This plastic fraction presents a significant challenge to recycling WEEE and WIEC, mainly because these wastes have a mixture of different types of plastic used for each component, presenting diverse mechanical properties [11]. The energy recovery from these wastes in our current and urgent decarbonization scenario becomes extremely important because their plastic component has a very significant calorific value, and their valorization represents one of the many value chains with potential to fit the global need of a circular economy.

Among the various technologies to recover energy from wastes, thermochemical conversion processes present greater flexibility in feedstocks and final products compared to other renewable technologies such as solar, hydro, and geothermal. In general, thermochemical technologies have as by-products solid material (biochars), liquid (bio-oil), and gases (syngas), which can be directly applied in energy production or be further used in various industries (e.g., chemical industry) [12–14].

While several studies have been conducted on thermochemical recovery technologies for different wastes (particularly biomass wastes or municipal solid wastes), WEEE or WIEC-based research is still in its beginning. Research topics are mainly focused on recycling [15,16], material recovery [7,17–19], environmental analysis [20], and waste characterization [15]. Few studies have focused on energy recovery through thermochemical methods, especially pyrolysis [15,16], carbonization [17–19], and gasification [20].

Thermal gasification is considered the most promising thermochemical technology for waste conversion [21]. This process converts the solid carbonaceous feedstock into a combustible gas (known as syngas) at high temperatures in the presence of a gasifying agent (e.g., air, oxygen, steam, CO_2, or mixtures of these agents) [22]. Syngas is mainly composed of CO and H_2, and it is a low-density, high-quality gas that can be further converted to liquid fuels (e.g., via the Fischer-Tropsch process) or heat and energy for power generation units [23].

Co-gasification is a way to produce syngas by simultaneously converting different feedstocks with varying characteristics. It has been proposed as a viable pathway to avoid issues that generally arise during the gasification of a specific waste [24].

Several works on WEEE recycling are in the literature, considering various specific aspects. The recycling of non-metallic fractions of e-waste has been investigated [18], as well as the chemical recycling of brominated flame retardants (BFRs) to produce clean fuel

[25]. More recent techniques, such as supercritical fluids [26] and thermochemical treatments [27], have been studied to produce value-added products from these wastes. The great variability of WEEE means that each author studies a different type of electronic waste.

Steam gasification in the presence of molten carbonates is a promising way to recycle WEEE, as the plastics contained in this material can be converted into product gas that can be recycled, and the noble metals are left for further processing. In the process, organic halogen compounds can be recovered as safe and stable inorganic salts. Typical chlorine-containing polyvinyl chloride (PVC) WEEE plastic was studied by steam gasification in the presence of molten carbonates at a temperature of 625 °C. The dechlorination step was investigated by thermogravimetric analysis, differential thermal analysis, and vapor gasification. The thermal decomposition of PVC occurred in two stages, the first stage being dechlorination in the low-temperature region around 200–400 °C, and the second stage being the decomposition of the remainder of the first stage. Dechlorination in steam gasification was mainly affected by steam flow, temperature, and carbonates [28]. Yamawaki T. (2003) evaluated the thermal gasification process for WEEE plastics containing brominated flame retardants. In this study, it was observed that in tests carried out at temperatures above 1200 °C, it is necessary to shock cool the gases to a temperature of less than 200 °C to suppress the emissions associated with brominated dioxins and chlorinated dioxins. The gas produced can then be used to generate heat or energy [29]. Combined pyrolysis-gasification tests were carried out using a two-stage reaction system to produce hydrogen by Acomb et al. (2013). Initially, the WEEE was pyrolyzed at 600 °C and the gases released during pyrolysis passed directly to a second reactor at 800 °C and reacted with steam in the presence of a mixture of Ni/Al_2 catalysts. This process increased the decomposition and yield of hydrogen [30].

WIEC can have significant amounts of chlorine and are very heterogeneous, making their direct conversion difficult in the thermal gasification process. Applying the carbonization process to these wastes can represent a pre-treatment solution to achieve better gasification performances. Carbonization promotes devolatilization of the material, making the gasification process of the carbonized material (char) produce less tar. The devolatilization process improves the C/H and C/O ratios of the feedstock and increases its reactivity, thus contributing to greater syngas production. In addition, the higher concentration of fixed carbon in chars makes the calorific value higher, and the higher the char production temperature, the higher the gasification heating rate [31,32]. The complexity of the gasification process requires the use of appropriate kinetic models to describe the different reactions and mechanisms of the process. Due to their enhanced physical-chemical properties, chars, particularly waste-derived chars, have been increasingly studied as feed for the gasification process [33].

Studies involving the carbonization (pyrolysis) of WEEE have been carried out by several researchers [34–36]. For example, the pyrolysis process has been widely studied for treating WEEE plastics and has been shown to be a viable process for the degradation and fixation of Br. Conventional pyrolytic degradation at temperatures below 500 °C of Br can result in a gas, liquid, and residue stream. However, when temperatures exceed 500 °C, Br is released in the gaseous form of HBr [37–40]. Halogen-laden WEEE plastics at high temperatures produce inorganic hydrogen halides (HCl and HBr). It is necessary to remove BFRs from WEEE plastics before the pyrolysis process. However, in most cases, this is not feasible due to economic or technical limitations and because they are covalently bound to the chain of polymers such as polyethylene (PE) [41,42]. The gas from the pyrolysis process is composed of hydrocarbons, and due to the presence of oxygen in the polymer structure, CO and CO_2 are also produced. The gases produced at temperatures above 500 °C contain HBr and light organic components such as bromomethane [35,40].

Marino et al. (2022) carried out pyrolysis tests on WEEE plastics containing PE and PVC using ZSM-5 zeolite and evaluated the performance and quality of oil production. In order to conduct the tests, carbonization at 350 °C was performed as a pre-treatment to eliminate chlorine from the raw material. The experiments involved using three samples of zeolites with varying levels of acidity, a downdraft fixed-bed stainless steel reactor, and temperatures of 600 °C and 450 °C in the thermal and catalytic zones, respectively. The tests concluded that adding ZSM-5 zeolites increased the oil and gas yields and enhanced the biochar's chlorine concentration [43].

Wang et al. (2023) studied the effect of temperature on the gasification process of biochars with a mixed atmosphere of CO_2 and H_2O using a batch reactor with temperatures varying between 750 and 1300 °C. They found that it is possible to control the chemical reaction and diffusion. The syngas results indicated that, in the competitive mechanism, both the char-CO_2 reaction and the char-H_2O reaction were inhibited [44]. Using the macro- Thermogravimetric Analysis (TGA) is one of the ways to obtain information regarding the general reaction kinetics in thermochemical conversion processes. Skreiberg et al. (2011) used TGA and macro-TGA to investigate kinetic mechanisms involved in thermal decomposition. TGA analyzes are performed on small, fine samples and milligram amounts. It is possible to determine the kinetics of the material due to the negligible mass and heat transfer resistance. The macro-TGA uses larger particles and a more significant amount of biomass and considers the limitations of the effects of mass and heat transfer affecting the overall decomposition of the process [45].

Fernandez et al. (2019) studied agro-industrial residues in macro-TGA with different heating rates (5, 10, and 15 K/min), controlling the release of CO. A comparison was made between the results of macro-TGA and TGA carried out previously with the same waste. In this study, the authors indicated that the reaction takes place in three well-defined stages, namely the evaporation of water, the devolatilization of the biomass, with the highest CO emissions, and the gasification of the biochar in the final stage [46]. Zhou et al. (2015) used macro-TGA to assess the behavior of hemicellulose, cellulose, and lignin during pyrolysis and found that several parallel reactions occurred [47]. Meng et al. (2015) and Long et al. (2017) studied the behavior of different components (biomass, pectin, starch, PE, polystyrene (PS), PVC, and polyethylene terephthalate (PET)) in the pyrolysis and gasification process [48,49].

The present study aims to contribute to understanding the thermal behavior of chars derived from waste biomass and WIEC mixtures. While previous studies have extensively focused on the thermochemical characterization and conversion of biomass and various components of WEEE, there remains a significant gap in the literature regarding the behavior of mixed waste feedstocks, particularly mixtures of biomass and WIEC, during thermochemical processes. Specifically, the interactions between these different types of wastes during thermal conversion, and how these interactions influence the overall efficiency and product distribution, have

not been adequately explored. This study seeks to elucidate the characteristics of these chars, providing insights into their thermal stability and decomposition behavior. Additionally, by employing macro-TGA to simulate conditions akin to a thermal gasification unit, this research provides a practical evaluation of these chars' behavior in real-world settings. Such an evaluation is essential for understanding and optimizing the co-gasification process of mixed waste streams, thereby unlocking the potential valorization of these wastes through thermal gasification and contributing to sustainable energy production and waste management.

2. Materials and methods

2.1. Feedstock

The WIEC sample used in this work was provided by a Portuguese company that recycles electrical cables to remove noble materials, with the WIEC being waste from this recycling operation. This material was mainly composed of polypropylene (PP), polystyrene (PS), and polyvinyl chloride (PVC). The waste lignocellulosic biomass (WLB) sample was provided by a company that manages waste from biomass in Portugal, and it mainly comprised pine wastes.

2.2. Carbonization experiments

The carbonization experiments were performed based on the tests previously carried out by Mota-Panizio et al. [50], using temperatures according to Nobre et al. [51]. The mixture used for the tests was composed of 50 % of WIEC and 50 % of WLB. Briefly, 15 kg of the mixture was placed in lidded clay pots and heated at a heating rate of 10 °C/min to the established carbonization temperatures (300, 350, and 400 °C) with a residence time of 2 h. For the carbonization tests, an electric furnace (Fornoceramic KS 72L) with a capacity between 12 and 20 kg per test, depending on the properties of the raw material, was used. The oven has a temperature and heating rate control panel and a capacity of 72 L in the carbonization zone.

After the carbonization process, the samples were grounded and sieved, with a particle size ranging from 75 to 3000 μm. The larger particles corresponded to the rubber material and larger pieces of metal that agglomerated during carbonization.

The biochars, which corresponded to the particles smaller than 425 μm (after sieving), were washed in heated water to remove soluble compounds and their improvement was evaluated [52,53]. For the washing process, the biochars were mixed with water and placed in glass containers with a ratio of 100 g/200 mL. The water was heated to a temperature of 95 ± 5 °C and the biochars were stirred for 30 min. After this process, the biochars were allowed to cool to room temperature, filtered, and dried in an oven (Holelab) at 105 °C for 24 h [53,54]. Biochar samples were named B300, B350, and B400 (in which B stands for " biochar", and 300, 350, and 400 correspond to the temperature at which the biochars were produced). The mass yield of the carbonization process was calculated according to Equation (1).

$$Mass\ yield\ (\%, db) = \frac{m_{biochar}}{m_{feedstock}} \times 100 \quad (1)$$

Where $m_{biochar}$ is the mass of the produced biochar and $m_{feedstock}$ is the mass of the feedstock used in the carbonization experiments.

2.3. Biochar characterization

2.3.1. Ultimate analysis

The concentrations of carbon, hydrogen, nitrogen, sulfur were determined using a Thermo-Fisher Scientific Flash 2000 CHNS-O analyzer. Oxygen was determined by difference and all samples were performed with replicates. The presented results correspond to average values and corresponding standard deviations.

2.3.2. Thermogravimetric analysis (TGA)

Thermogravimetric analysis was used to determine proximate analysis (moisture content, volatile matter, fixed carbon, and ash). Tests were performed in triplicate with sample weights between 3.5 and 4.5 mg. To minimize the associated errors, the samples were grounded and homogenized. A PerkinElmer STA 6000 thermogravimetric analyzer was used, with a heating rate of 20 °C/min in an oxidative atmosphere. Proximate analysis of each biochar was determined from the thermogravimetric profile (variation of sample mass versus temperature), considering the inflection points of the mass derivative in function of time. The derivative is obtained from the equipment, which has the DTG option based on the test carried out.

The combustion characteristics of biochars can be evaluated through the ignition index (D_i) and the comprehensive combustibility index (D_c), which are defined according to Equations (2) and (3).

$$Di = \frac{DTG_{max}}{T_f \times T_i} \quad (2)$$

$$D_c = \frac{DTG_{max} \times DTG_{mean}}{T_b \times {T_i}^2} \quad (3)$$

Where, T_i is the ignition temperature (°C) corresponding to the beginning of mass loss and is defined as the temperature the mass loss

rate reaches after the initial peak of moisture loss in the DTG profile; T_b is the burnout temperature (°C), it is identified when the last peak reaches the end and corresponds to the temperature at which the sample is completely oxidized; DTG_{max} is the maximum rate of mass loss (mg), and can be found from the point where the maximum reaction rate occurs at T_{max}; T_f is the temperature according to the maximum mass loss rate (°C); The DTG_{mean} is the average rate of mass loss (mg/min) [55,56]. These values can be identified in the TGA/DTG graphic, as shown in Fig. 1, where the dashed line corresponds to mass loss as a function of temperature (TGA) and the solid line is the derivative (DTG). The peaks identify the drying, devolatilization, and combustion zones, in addition to the previous data.

2.3.3. High and lower heating value

The high heating value (HHV) of the samples was determined using a bomb calorimeter (IKA C 2000), which performs the analysis through the complete combustion of the samples in an adiabatic environment. For HHV determination, 0.5 ± 0.1 g of each sample (dry) was placed in the equipment and its total combustion was carried out. The calculation of the lower heating value (LVH) was carried out according to Boie's equation, as shown in Equation (4):

$$LHV_{Biomass} = 34.8C + 93.9H + 10.5S + 6.3N - 10.8O \quad (4)$$

2.3.4. Chlorine content and mineral composition

The amount of chlorine present in the biochar sample was determined by X-ray fluorescence (Thermo Scientific Niton XL 3T GoldD + analyzer).

Mineral composition of the biochars was determined through ICP-AES (Horiba Jobin-Yvon Ultima). Slagging (B/A) and Fouling (Fu) indexes were determined according to Equations (5) and (6), respectively [58,59]:

$$B/A = \frac{Fe_2O_3 + CaO + MgO + K_2O + Na_2O}{SiO_2 + TiO_2 + Al_2O_3} \quad (5)$$

$$Fu = B/A \; x \; (Na_2O + K_2O) \quad (6)$$

2.4. Macro-TGA experiments

The thermal gasification reactor simulation tests were performed in a macro-TGA equipment consisting of an in-house 2 kW ceramic furnace (Fig. 2). This equipment reaches temperatures of 0–1200 °C, with chamber dimensions of 200 mm in diameter and 350 mm in height. For the tests, an analytical scale (Skinko Denshi AJ-620CE) with a precision of 0.001 g was suspended on the top of the unit and the data was acquired in real time using LabView. This system also has a carrier gas system from a high-pressure gas cylinder and a TSI 4043 G air flow control system, which regulates the gas flow control during experiments. Continuous calibrations were performed during the execution of the experiments. The oven was heated to working temperature and each sample was manually loaded into an aluminum basket and placed in the constant temperature zone.

The gases produced during the experiments were collected and passed through a gas washer system by bubbling and a cotton filter to remove particles and moisture. The gases were subsequently analyzed by a portable analyzer (Rapidox 5100 Syngas Analyzer) connected in line with the reactor. The portable gas analyzer has a gas inlet volume system of 1 L/min, a maximum pressure inlet of 10 bar, and temperature of 50 °C. CO, CH_4, CO_2, and O_2 gases are detectable by IR and H_2 by a TCD sensor.

Table 1 shows the conditions under which the macro-TGA tests were performed.

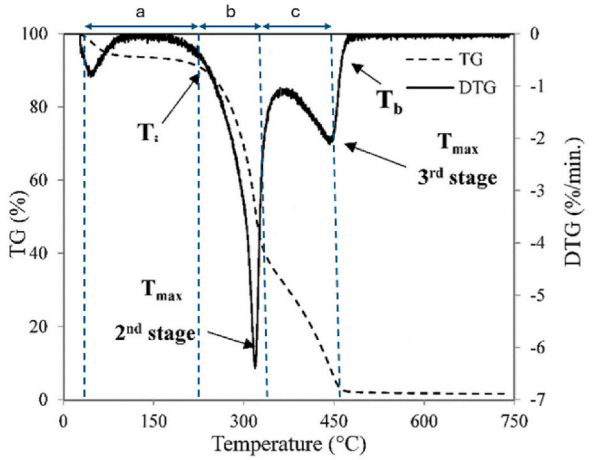

Fig. 1. Interpretation of thermogravimetric analysis results: a) drying stage, b) devolatilization, and c) char combustion [57].

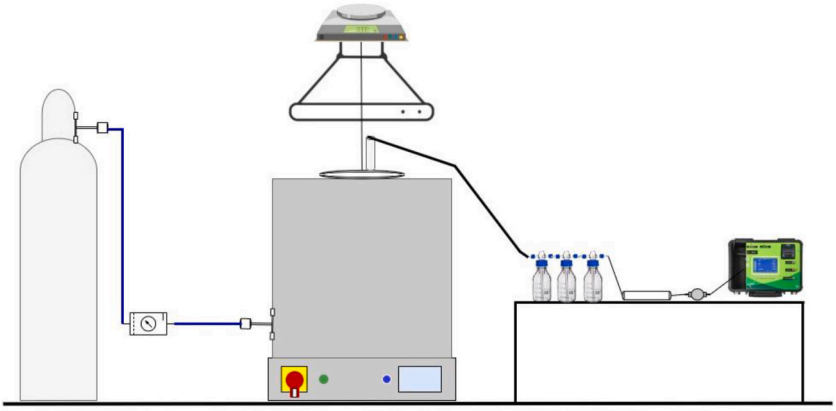

Fig. 2. Macro-TGA testing system, coupled with gas cleaning system and portable syngas analyzer for thermal gasification.

Table 1
Macro-TGA test conditions.

Test	Equivalence ratio (ER)	Temperature (°C)	Initial mass (g)
B300-750	0.3	750	19.698
B350-750	0.3	750	20.507
B400-750	0.3	750	20.314
B300-800	0.3	800	19.552
B350-800	0.3	800	20.423
B400-800	0.3	800	20.644
B300-850	0.3	850	20.135
B350-850	0.3	850	20.058
B400-850	0.3	850	20.404

2.4.1. Gasification performance in macro-TGA simulations

In order to assess the performance of macro-TGA tests, the LHV of the syngas was calculated according to Basu 2013 [67] (Equation (7)), using the proportion of each gas (%) that makes up the syngas:

$$LHV\left(\frac{Mj}{Nm^3}\right) = (63.41C_2H_4) + (70.29C_2H_6) + (58.06C_2H_2) + (25.10H_2S) + (38.82CH_4) + (12.63CO) + (12.74H_2) \quad (7)$$

The calculation of the cold gas efficiency (CGE) is important in studying the gasification process. Theoretically, the lower the gassing temperature, the higher the CGE will be, but the low temperature causes problems related to emissions and a decrease in the gassing rate [60]. In this work, CGE was calculated using Equation (8) [61]:

$$\eta_{CGE} = \frac{V_{syngas} \times LHV_{syngas}}{m_{drybio} \times LHV_{drybio}} \quad (8)$$

Where V_{syngas} is the volume of syngas produced (m^3/h); LHV_{syngas} is the lower heating value of the produced syngas (MJ/m^3), m_{drybio} is

Table 2
Characterization of raw materials (WLB and WIEC) and corresponding biochars obtained at 300 °C (B300), 350 °C (B350) and 400 °C (B400).

Parameters	Units	Samples			
		WLB/WIEC (1:1)	B300	B350	B400
Moisture	wt.%, ar	4.26	6.22	6.17	3.69
Ash	wt.%, daf	27.5	33.40	33.60	34.00
C		44.91 ± 0.66	42.38 ± 3.26	43.06 ± 6.98	43.14 ± 3.83
H		5.20 ± 0.44	2.81 ± 0.64	3.33 ± 0.73	3.76 ± 1.07
N		1.25 ± 0.13	12.9 ± 0.19	11.38 ± 0.21	10.41 ± 0.02
S		< DL	< DL	< DL	< DL
O		21.14 ± 0.82	8.51 ± 1.32	8.63 ± 4.8	8.69 ± 0.67
HHV	MJ/kg, db	21.23	19.60	19.67	19.71
LHV		18.42	18.08	17.87	17.68
Cl	mg/kg, db	15.03	2.48	2.28	2.58

Note: ar – as received basis; daf – dry ash free basis; db – dry basis; DL – Detection Limit.

the mass of feedstock (biomass or biochar) consumed during the tests (g), and LHV_{drybio} is the lower heating value of the feedstock (MJ/kg).

Carbon conversion efficiency (CCE) describes how much of the total carbon in the fuel used is converted into carbon-containing product gases such as CO, CO_2, CH_4. The CCE is given by Equation (9):

$$CCE = \frac{(\%CO + \%CH_4 + \%\ CO_2)}{(22.4 \times \%C_{bio})} \times 100 \quad (9)$$

Where % CO, % CH_4, and % CO_2 are the volumetric concentrations of carbon monoxide, methane, and carbon dioxide (%), and $\%C_{bio}$ is the percentage of carbon present in the feedstock.

3. Results and discussion

3.1. Feedstock and biochar characterization

The results obtained in the characterization tests of the raw materials used in the carbonization process and corresponding biochars are shown in Table 2.

In biomass and wastes submitted to thermochemical processes such as carbonization, the devolatilization conditions play an important role in the kinetics of the processes, thus affecting the biochar yield and its reactivity [62]. The mass yields of B300, B350, and B400 were 72.20 %, 70.69 % and 72.24 %, respectively.

One of the most notable features of the produced biochars is the increase in ash content with increasing production temperature. This is usual in char production, as organic matter is volatilized, and the mineral components remain in the char matrix [63]. These ash content values could represent a significant application constraint if the final usage of these chars were to be a combustion process. This is related to a higher probability of slagging and fouling phenomena [64] as well as a reduction in the HHV of the biochars [65].

Regarding ultimate composition, Table 2 shows that the carbon content of the biochars produced at 300, 350, and 400 °C remains relatively stable (42.38 %–43.14 %) due to the similar initial carbon content of the feedstock and the narrow temperature range, which does not significantly alter the extent of carbonization or decomposition of carbon-containing compounds. On the other hand, nitrogen

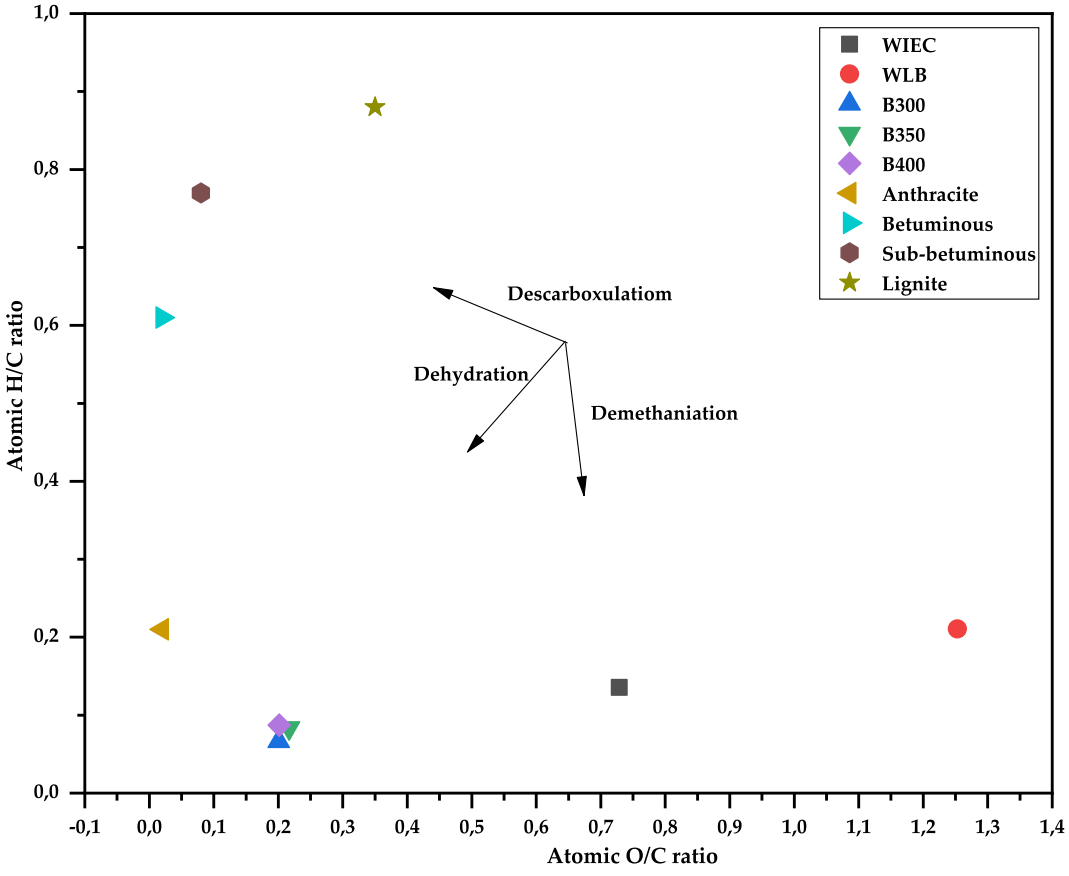

Fig. 3. Van Krevelen diagram for the raw materials and biochars produced.

increased substantially in all biochar samples. Some nitrogen-containing compounds may undergo stabilization during the carbonization process, resulting in the concentration of nitrogen increasing in the biochar. This stabilization process involves the transformation of labile nitrogen compounds into more recalcitrant forms, that are resistant to further decomposition [66]. The HHV of the produced biochars is lower than the HHV of the original feedstock. This result can be related to the loss of volatile components, changes in chemical composition, inefficiencies in carbonization, and the loss of energy-rich components during the carbonization process [67].

The decomposition of PVC does not significantly affect energy concentration but reduces the amount of oxygen and chlorine in the final biochars through gaseous products. With the increasing temperature, the amount of chlorine in the biochars tends to increase due to the elimination of volatile matter during this process [50]. The surface of the biochar is highly heterogeneous, and in addition to the aromatic structure, it has polar groups that can establish bonds with the chlorine ion retained in its structure [68]. Chlorine content in biochar often exceeds 1 %, causing equipment corrosion. Water washing pre-treatment is an effective way to remove chlorine and it affects the properties of fuels. It can remove up to 80 % of Na and Cl [69].

Fig. 3 shows the Van Krevelen diagram for the original feedstock and the produced biochars, using fossil solid fuels for comparison.

Comparing the biochars with the raw materials, it is possible to assess a more accentuated reduction in the O/C ratio and the H/C ratio, which indicates that the material underwent dehydration and decarboxylation reactions which are intensified in biochars and with higher production temperatures [70,71].

Biochars showed increased similarities with fossil fuels, being positioned between lignite and sub-bituminous coal, with B300 being closer to sub-bituminous coal. These results show that the produced biochars have a relatively low degree of oxidation (O/C ratios less than 0.3) and a more significant amount of unsaturation (H/C ratios less than 0.5) [72].

Fig. 4 shows the data on the mineral composition of the biochar samples, and Fig. 5 shows the results for the calculations of the slagging (B/A) and fouling (Fu) indexes.

The mineral composition of the biochars has a significant impact on further thermochemical processes and the quality of value-added by-products [73,74]. Ash-related problems, including slag and corrosion, can degrade equipment and reduce process performance. The encrustation of ash and slag caused by inorganic compounds (K, Na, Ca, Mg, Si, Cl, S, and P) increases the risk of ash deposits forming on the heat transfer surface and slag accumulating at the bottom of reactors [75]. Problems related to surface heat are mainly caused by the presence of silica, chlorine, and sulfur [76]. High alkali and alkaline earth metals levels in ash, especially sodium,

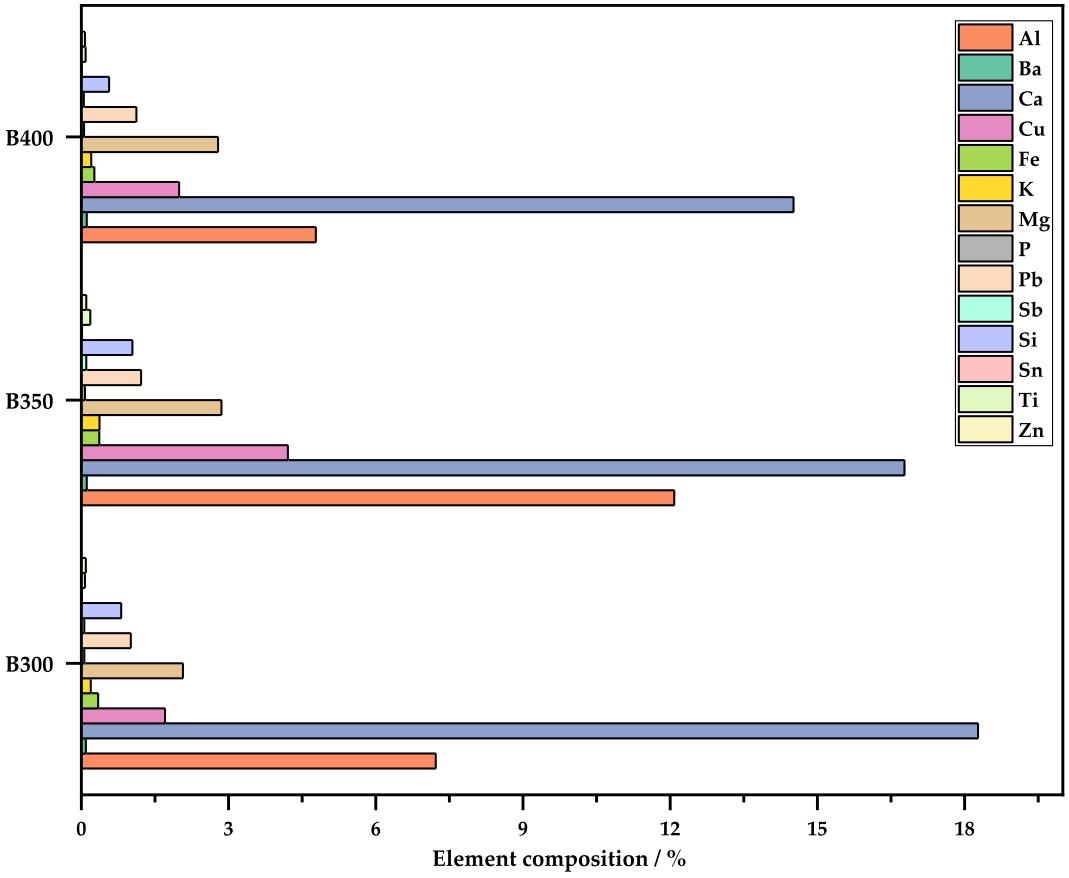

Fig. 4. Mineral composition of the produced biochars.

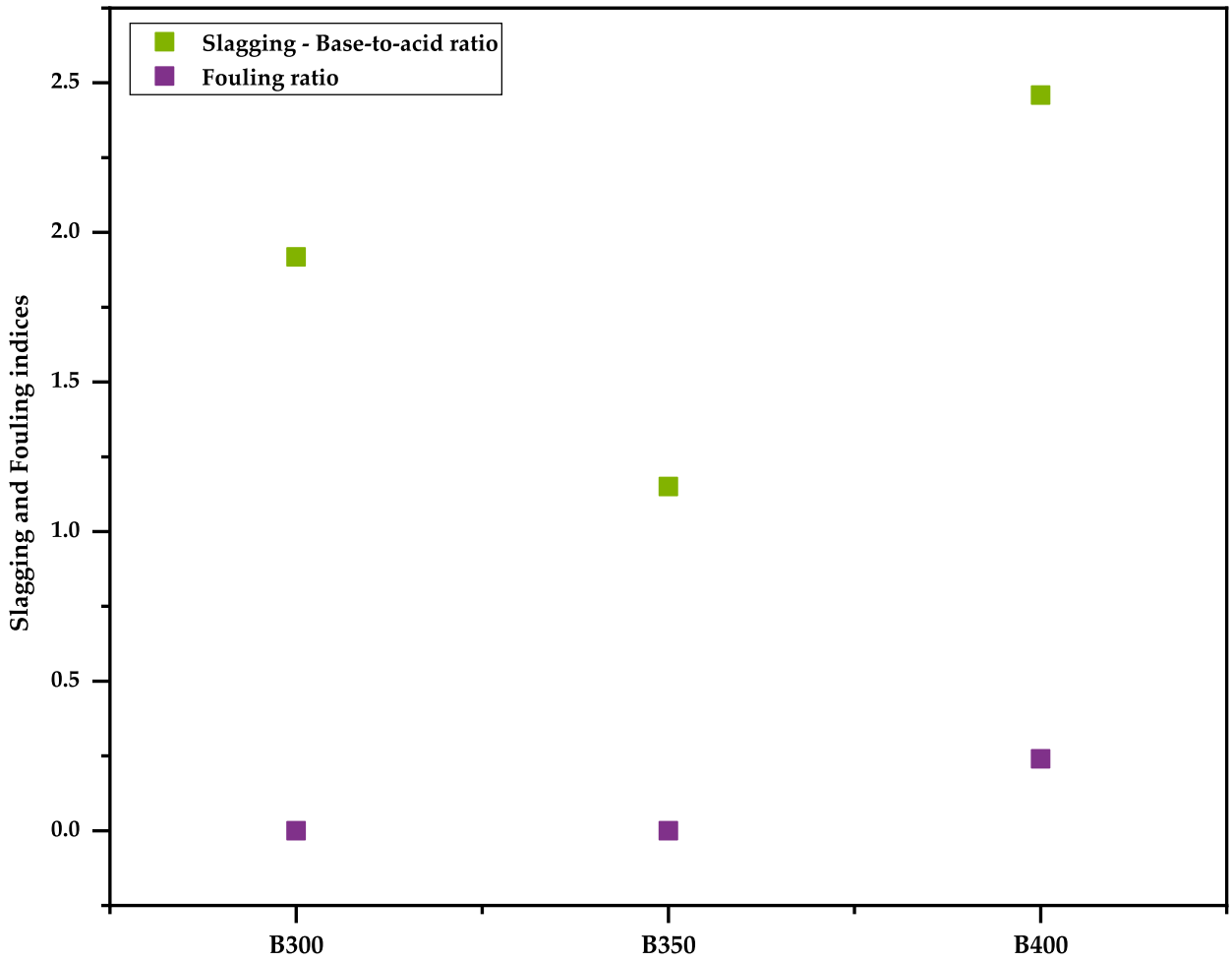

Fig. 5. Slagging and fouling indexes for the produced biochars.

potassium, magnesium, and calcium, can cause severe fouling and slagging problems [77,78]. Alkali metals in particular, have lower melting points than other elements usually present in biomass and waste mineral profiles, contributing to incrustation and slagging phenomena [79].

Fig. 4 shows that calcium, aluminum, copper, and magnesium are in higher concentrations in the produced biochars, whereas lead and silica present the lowest concentrations. The amount of sodium present in the biochars is below 0.01 %, which is an important factor that is reflected in the calculations for the Fu index. Slagging and fouling reduce boiler efficiency and endanger the safe operation of the unit [80]. According to the values calculated for the B/A, these samples present a high potential for slag formation, while the Fu indicates that the ash has a low propensity for fouling formation. According to the literature, B/A values below 0.5 have a low tendency to form slag, 0.5–0.7 have a medium tendency, and 0.7 have a high probability of slag formation [81]. With regard to Fu, the probability of fouling is low if the value is less than 0.2, medium if the value is less than 0.5, and high if the value is above 1 [82].

TGA and DTG profiles can determine the main parameters for burning, such as weight loss rate, burning temperatures, sample reactivity, and combustibility, which are used to predict thermal behavior [83,84]. TGA and DTG profiles for the biochars produced at temperatures of 300, 350, and 400 °C after the hot water washing process were conducted. For the profiles, heating rates of 10 °C.min^{-1} (Fig. 6), 30 °C.min^{-1} (Fig. 7), and 50 °C.min^{-1} (Fig. 8) were used.

In the DTG profiles, it is possible to observe three different peaks corresponding to the various stages of degradation of the material, namely dehydration (drying), devolatilization, burning of fixed carbon (char combustion), and mineral decomposition. The first peak of mass loss is dehydration with temperatures up to 150 °C, corresponding to the moisture in the biochars. It is associated with the washing process but also with the relative air humidity. The second peak of mass loss corresponds to devolatilization, up to 520 °C, and it is considered the burning of volatile matter still present in the biochar samples. The structural components of biomass, namely cellulose (250–300 °C) and hemicellulose (200–300 °C), are practically degraded during the biochar production. However, lignin (200–500 °C) shows its decomposition in this second peak [85]. The third peak of mass loss, between 520 and 790 °C, corresponds to fixed carbon. The remaining samples are associated with ash, the mineral decomposition of the material that was not burned [86,87]. Furthermore, it is possible to observe that the higher the heating rate, the greater the peak intensity and the smaller the difference

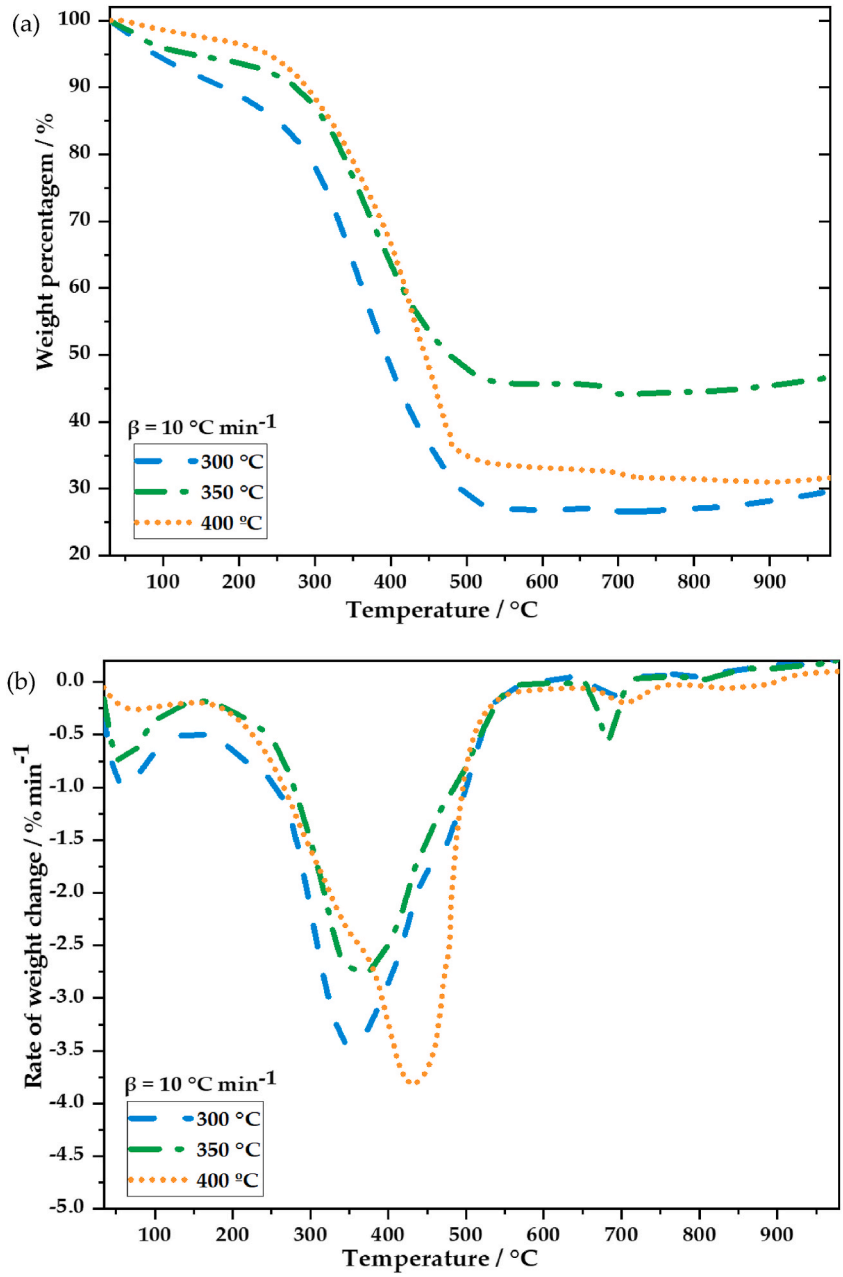

Fig. 6. TGA (a) and DTG (b) curves of biochars with a heating rate of 10 °C.min^{-1}.

between the different biochars. In DTG at a rate of 10 °C.min^{-1} it is possible to verify that the greatest degradation of volatiles occurs after the temperature of biochar production. However, at a heating rate of 50 °C.min^{-1}, it is possible to observe that the heating rate is high, and the most significant degradation occurs at 450 °C.

In the TGA profile with a heating rate of 10 °C.min^{-1} it is possible to observe that with the increase in the carbonization temperature, the amount of ash in the biochar increases. This is because the higher the temperature, the greater the amount of volatiles degraded in the biochars, a factor intensified by the fact that the biochars were washed and compounds on the biochar surface were removed. This difference is no longer apparent as the heating rate increases because the reaction speed is faster.

The ignition temperature (Ti) and the burnout temperature (Tb) increase as the biochars' production temperature rises (Table 3). A high Ti shows that the material is technically more stable, which makes it more difficult to ignite, while a high Tb makes it more difficult for the material to burn, leading to a longer residence time and, consequently, an increase in temperature to complete the conversion. Low ignition and burnout temperatures show greater reactivity.

In addition, DTG_{mean} decreased with increasing reaction temperature, attributed to the lower amount of volatile matter in the

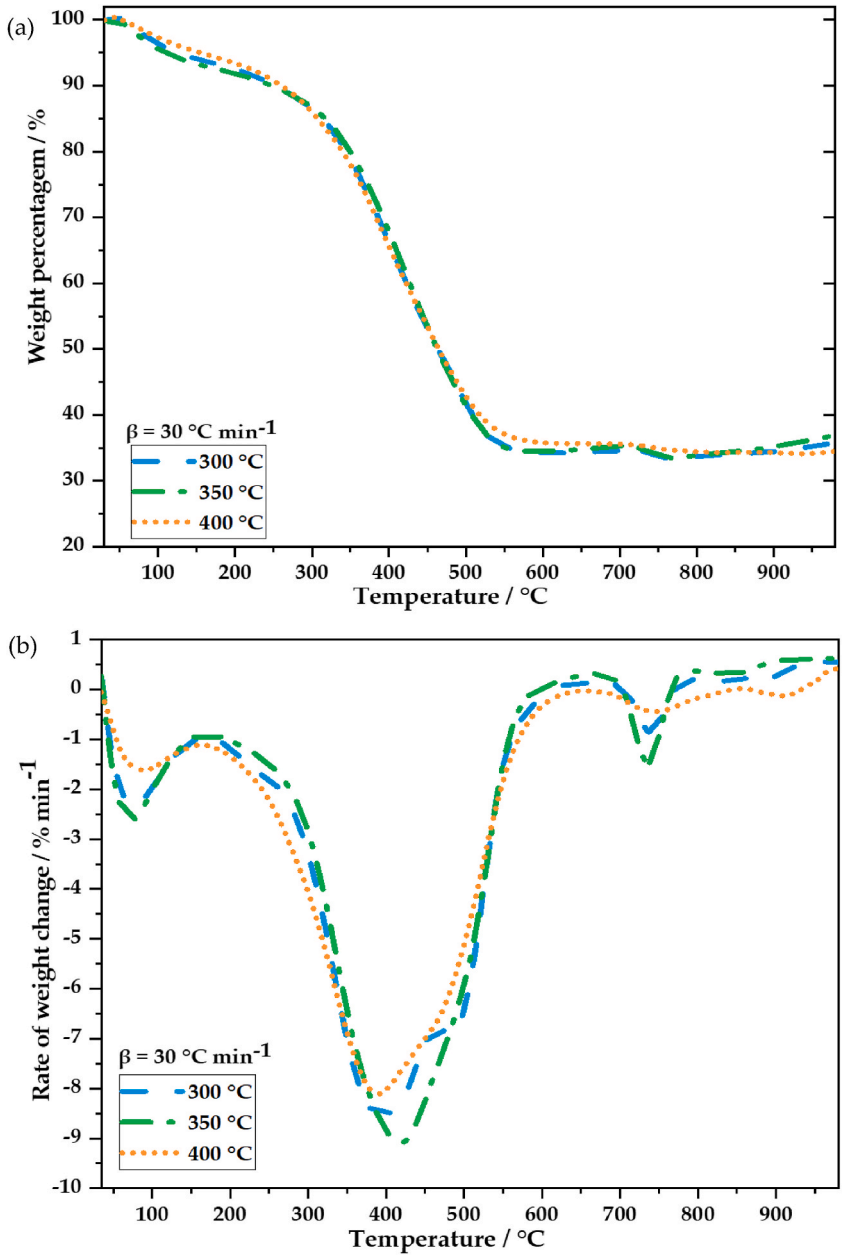

Fig. 7. TGA (a) and DTG (b) curves of biochars with a heating rate of 30 °C.min^{-1}.

biochar. The D_i and D_c of the biochars also followed the tendency to decrease with the increase in the temperature at which the biochar was produced, also associated with the amount of volatile matter present, since the greater the amount of ash, the greater the effects of limiting mass transfer during the conversion process.

3.2. Macro-TGA tests

Fig. 9 shows the mass loss thermographs concerning the residence time inside the macro-TGA reactor.

TGA analyses are carried out using small, thin biomass samples. Resistance to heat transfer and mass are not significant, so the kinetics of individual particles can be obtained. Compared to macro-TGA, the sample size and particle sizes are larger, so the effects of heat and mass transfer affect the overall decomposition of the process. Thus, macro-TGA tests can provide helpful information regarding the behavior of biomass residues in commercial plants and the kinetic parameters will be apparent.

Under thermal gasification conditions, the highest percentage of mass loss occurs in the first 200–250 s. With a longer residence time, the degradation of the biochar begins to stabilize, with slight variation in weight. As the operating temperature increases, the

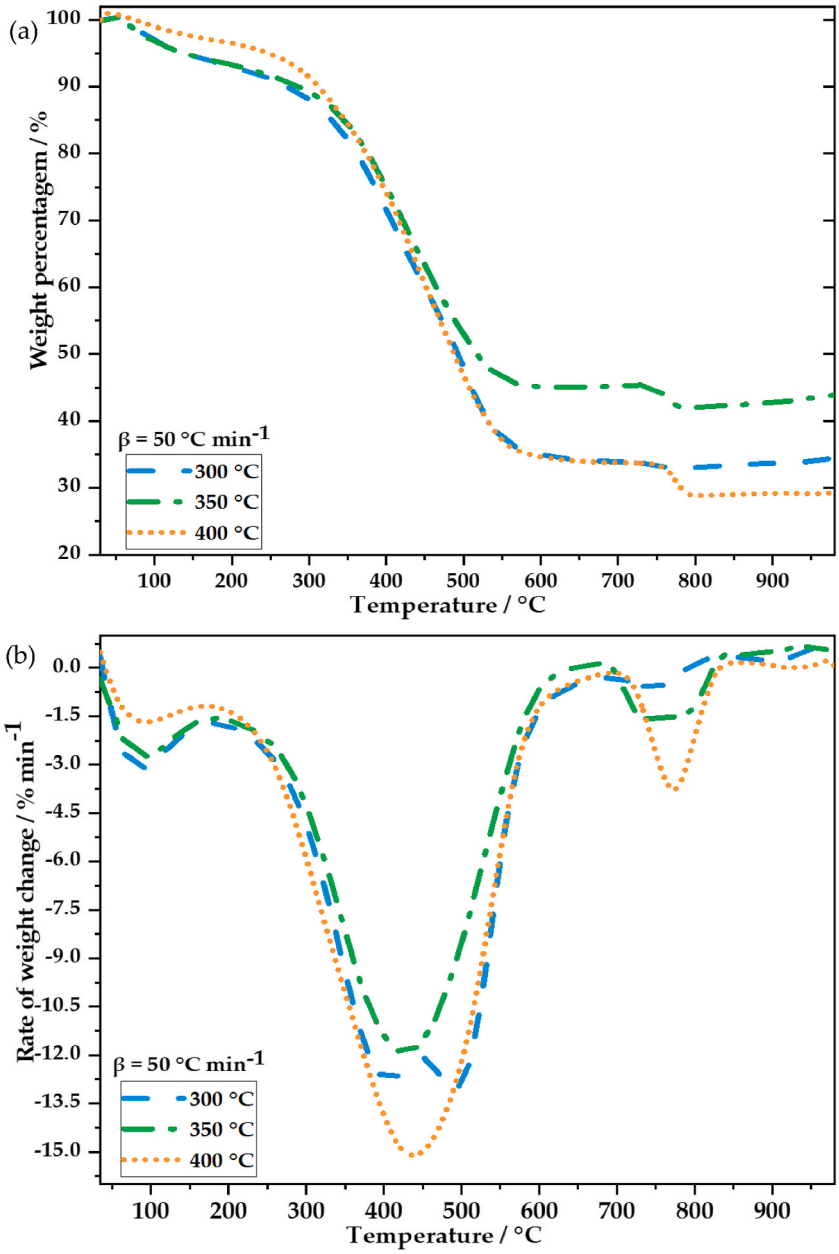

Fig. 8. TGA (a) and DTG (b) curves of biochars with a heating rate of 50 °C.min^{-1}.

Table 3
Characteristic parameters for biochars for T_i, T_b, T_{max}, DTG_{max}, DTG_{mean}, D_i, and D_c.

Sample	T_i (°C)	T_b (°C)	DTG_{max} (mg.min^{-1})	T_{max} (°C)	DTG_{mean} (mg.min^{-1})	$D_i x10^6$ (mg/min. °C^2)	$D_c x10^9$ (mg^2(min^2. °C^3))
B300	169.08	564.59	0.26	380.28	0.02	4.03	0.32
B350	186.67	565.65	0.20	384.70	0.02	2.77	0.15
B400	188.54	566.30	0.16	386.58	0.01	2.14	0.10

amount of sample is further reduced at the start of the process, thus increasing the reaction rate exponentially as the temperature rises.

According to Wu and Li (2023), the model they studied found that at lower sample temperatures, the difference between the maximum sample temperature and the furnace temperature is more significant, and the model reflects this difference. They found this

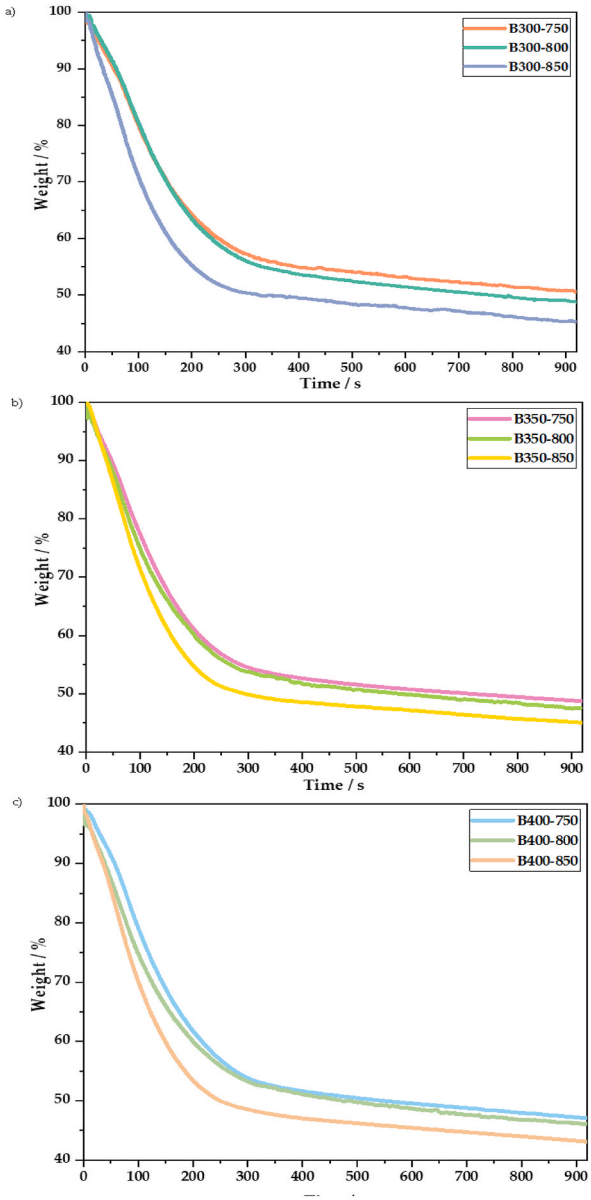

Fig. 9. Macro-TGA profiles of the thermochemical decomposition of biochars under gasification conditions: a) Sample B300 at 750, 800, and 850 °C; b) Sample B350 at 750, 800, and 850 °C and c) Sample B400 at 750, 800, and 850 °C.

reaction may be due to stronger heat radiation between the sample and the furnace at higher temperatures [88].

3.3. Syngas analysis

Syngas is mainly composed of H_2, CO, N_2, CO_2, H_2O, CH_4 and hydrocarbons. The specific final composition of syngas depends on the fuel source and the production technology. Factors such as equivalence ratio (ER), temperature, type of gasifying agent, pressure, residence time, and feed properties affect the performance of the gasification system [89]. Fig. 10 shows the syngas composition for each produced biochar (300, 350, and 400 °C) at the tested gasification temperatures (750, 800, and 850 °C).

As the amount of CO increases, more CH_4 and H_2 are formed through methanation [90]. According to Weiland et al. (2012), the yield of CH_4 is correlated with the gasifying temperature, and a temperature above 1400 °C is required to achieve CH_4 concentrations in low syngas (dry and free of N_2) [91]. The syngas data shown in Table 4 and Fig. 10 are for dry syngas and free of N_2 and O_2.

As the equivalence ratio is high, the oxidation process is accelerated, thus reducing the quality of the gas produced and the amount of CO_2 present in the gas is high, ranging from 60 to 74 %. Tests on biochar produced at 300 °C show that CO_2 production increases from 61 % to 72 % as the CO production temperature from the Boudouard reaction increases. Increasing the reactor temperature

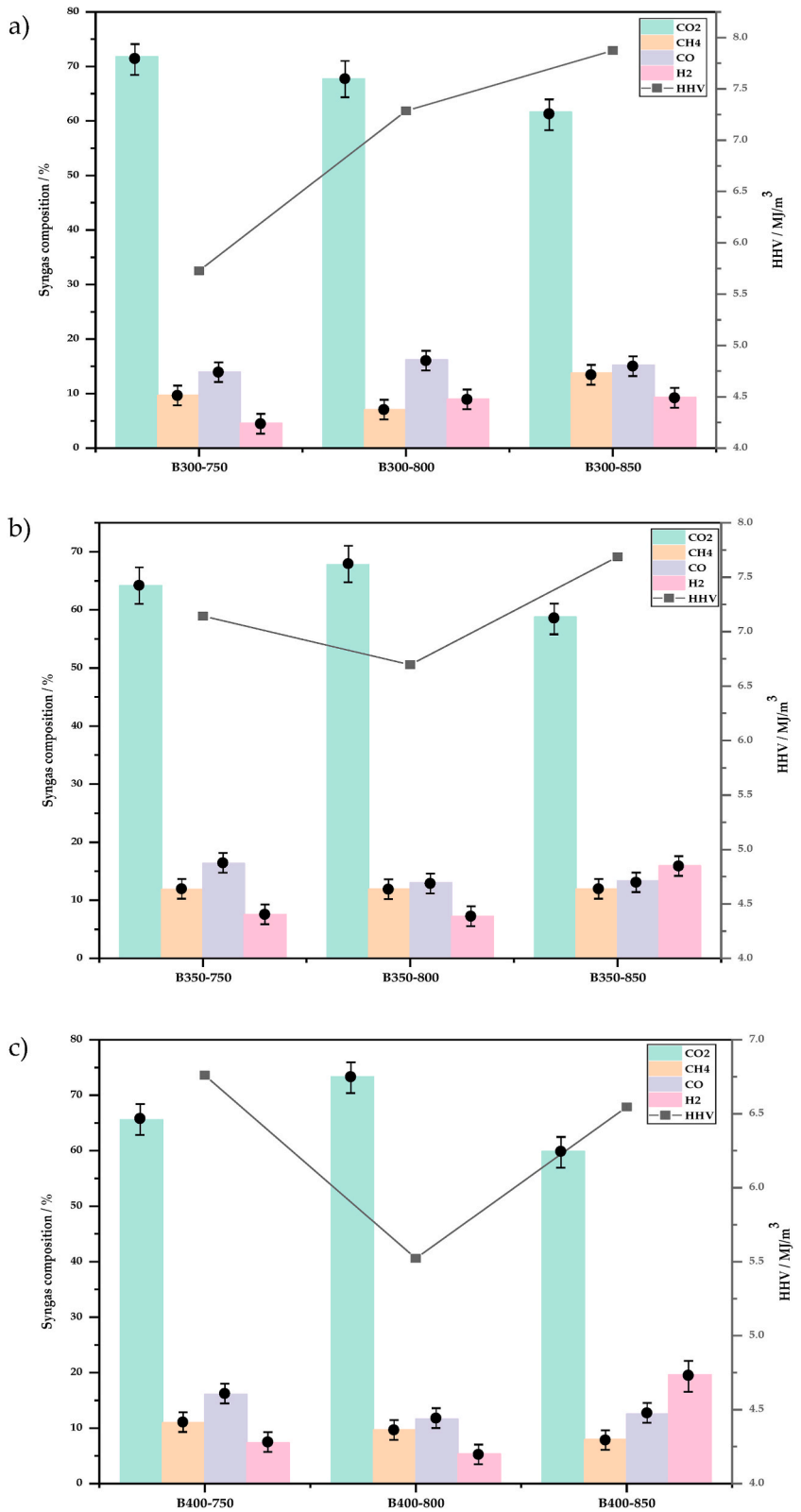

Fig. 10. Composition and heating value of the gas products produced during the thermochemical decomposition of the biochars in gasification conditions: a) B300, b) B350, and c) B400.

Table 4
H_2/CO, H_2/CH_4, and CO_2/CO ratios for the different gasification simulation tests using macro-TGA.

Sample	H_2/CO	H_2/CH_4	CO/CO_2
B300-750	0.33	0.47	0.19
B350-750	0.46	0.63	0.26
B400-750	0.46	0.67	0.25
B300-800	0.55	1.27	0.24
B350-800	0.55	0.61	0.19
B400-800	0.46	0.55	0.16
B300-850	0.61	0.68	0.25
B350-850	1.20	1.33	0.23
B400-850	1.56	2.47	0.21

causes the amount of hydrogen to increase, for B300 it increased from 4.6 % to 9.3 %, B350 from 7.2 % to 15.9 % and B400 from 7.3 % to 19.6 %. B400 has a higher hydrogen-to-carbon ratio, thus allowing for greater quantities of hydrogen in the syngas. In biochars B350 and B400 at a reactor temperature of 800 °C, it is possible to see a reduction in the volumetric content of H_2 (7.2 % and 5.3 %, respectively) and CO (13 and 11.6 %, respectively) caused by consumption during syngas formation, resulting in a reduction in calorific value and cold gas efficiency (CGE). The formation of CH_4 in the syngas means the consumption of H_2, and consequently, the concentration of H_2 in the syngas decreases. Syngas with stoichiometric H_2/CO ratios between 1 and 2 means that the syngas has favorable conditions for producing chemical products, such as methanol, ethylene, ethylene glycol, and other chemical products [92]. The H_2/CO and H_2/CH_4 ratios impact the combustion process and influence the laminar flame speed, thus providing important information regarding the shape and length of the flame. Table 4 presents the main results for syngas composition obtained in the macro-TGA test with the produced biochars.

In the gasification process, in the catalytic pyrolysis stage, it is beneficial to increase the H_2/CO ratio by increasing the production of H_2 and reducing the amount of CH_4 produced. In the macro-TGA tests at 850 °C with the biochars produced at temperatures of 350 and 400 °C, it was possible to see that the H_2/CO and H_2/CH_4 stoichiometric ratios increased, meaning a reduction in the amount of CH_4 produced in the gas and an increase in the percentage of H_2 in the gas, providing an improvement in the conditions of the syngas and higher calorific value. The higher amount of H_2 in the final syngas is desirable when the gas is used in energy conversion systems, thus increasing energy generation [93].

A low CO/CO_2 ratio significantly affects the composition of the product gas, the reaction time, and the reaction temperature,

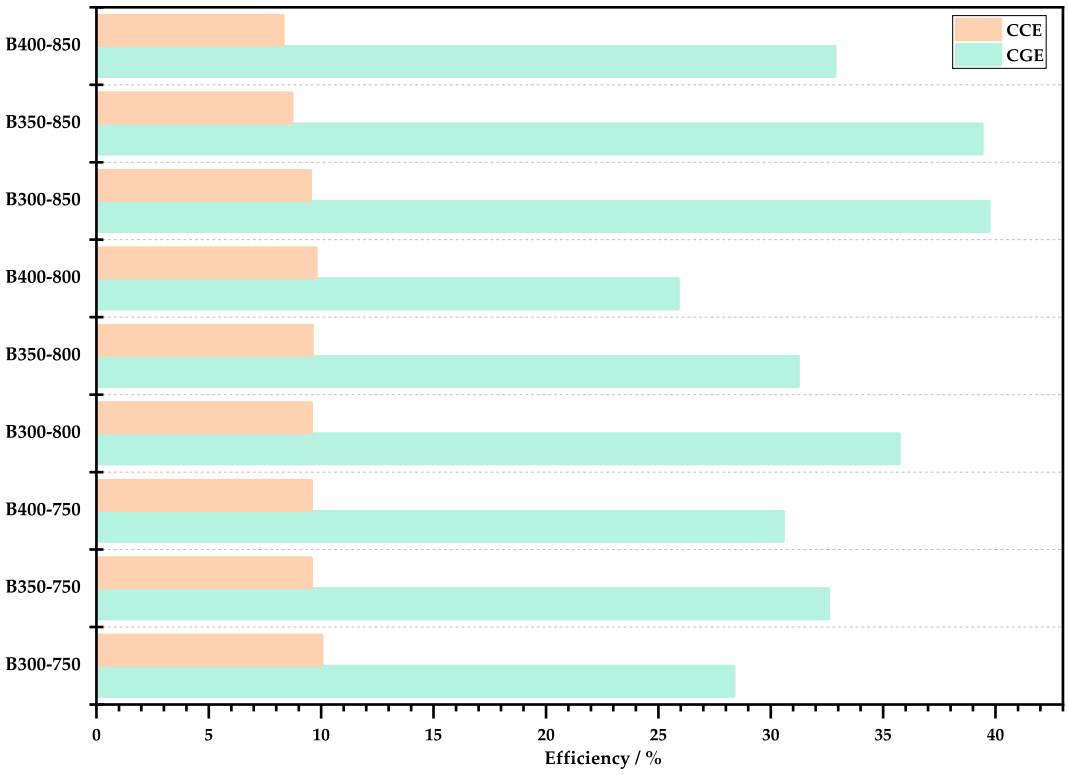

Fig. 11. Cold gas efficiency (CGE) and carbon conversion efficiency (CCE) in the macro-TGA tests.

correlating with the Arrhenius equation and increasing with operating temperature. However, the CO/CO_2 ratio strongly depends on the char's origin and treatment [94]. The carbonized biochars at 300 and 350 °C have higher CO/CO_2 ratios than those produced at 400 °C at 800 and 850 °C operating temperatures. According to Scala et al. (2009), biochars in the gasification process at 850 °C, the carbon in the biochar is oxidized to CO_2 and a reduced fraction to CO, thus causing lower CO/CO_2 ratios [95].

Fig. 11 shows the results obtained for cold gas efficiency (CGE) and carbon conversion efficiency (CCE) for the macro-TGA tests carried out with the produced biochars under gasification conditions.

The CGE is the ratio of the heat content present in the biochar to the heat content of the syngas produced under ambient conditions. It measures how efficiently the biochar energy is converted into energy for the syngas. According to Fig. 11, only 50 % of the biochar energy was converted into energy for the syngas. Li et al. (2017) carried out tests with air gasification and showed that the thermodynamic equilibrium predicts that the CGE is maximum in ER between 0.18 and 0.25 depending on the temperature used in the gasification process. They also observed that the peak occurs with ER between 0.25 and 0.35 [96]. As the ER increases, the carbon present in the biochars is converted into CO in the syngas. The energy produced is adequate to compensate for the dilution caused by the larger amount of N_2 resulting from the higher ER. Once all the carbon has been converted, the amount of N_2 combined with the syngas oxidation leads to a lower CGE. Another important factor for the CCE is related to the concentration of CO_2. With the increase in the ER, the amount of CO_2 also increases and acts as a reagent for reducing the amount of char. However, the amount of unreacted CO_2 acts as a diluent in syngas. Based on the results obtained through the macro-TGA, the CCE, CGE, and the amount of CO_2 in the syngas indicate that the thermal gasification of the biochars B300–850, B350-850, and B400-850 were the ones that presented the best results. The results also suggest that it is possible to reduce the amount of CO_2, increasing the calorific value and the H_2 in the product gas with higher temperatures.

4. Conclusion

This study analyzed the thermochemical decomposition behavior and gasification performance of biochars derived from woody feedstock and waste cable insulation blends at various temperatures. The characterization findings revealed that ash content rose significantly with increasing biochar production temperatures, reaching 34 % at 400 °C. This could pose challenges for combustion applications due to heightened risks of slagging and fouling.

Thermochemical decomposition profiles delineated distinct stages, with dehydration occurring up to 150 °C, devolatilization between 150 °C and 520 °C, and fixed carbon burning from 520 °C to 790 °C. Syngas analysis highlighted the impact of ER and reactor temperature on syngas composition, with higher temperatures favoring hydrogen-rich gas production. The observed trends in CGE ranged from 42.61 % to 50.40 % and CCE from 45.83 % to 50.40 %, underscoring the significance of temperature control in maximizing gasification performance and energy conversion efficiency. Biochars produced at higher temperatures demonstrated superior gasification performance, indicating the potential for optimizing biochar production processes to enhance energy recovery and waste valorization.

Overall, this study contributes to advancing the understanding of thermochemical conversion processes and provides valuable insights for optimizing biochar production and gasification systems, thereby fostering sustainable energy generation and waste management practices in biomass-based industries. Future research could explore additional process parameters and refine operational conditions to further increase gasification performance and energy conversion efficiency.

Funding

This work was supported by national funds through the Fundação para a Ciência e a Tecnologia, I.P. (Portuguese Foundation for Science and Technology) by project UIDB/05064/2020 (VALORIZA - Research Centre for Endogenous Resource Valorization) and project UIDB/04077/2020–2023 (MEtRICs - Mechanical Engineering and Resource Sustainability Center).

Ethical clearance

Not applicable.

Data availability statement

Data will be made available on request.

CRediT authorship contribution statement

Roberta Panizio: Writing – original draft, Visualization, Validation, Methodology, Investigation, Formal analysis. **Carlos Castro:** Investigation. **Nuno Pacheco:** Investigation. **Ana Carolina Assis:** Writing – original draft, Investigation. **Andrei Longo:** Writing – original draft, Investigation. **Cândida Vilarinho:** Resources, Methodology. **José Carlos Teixeira:** Resources, Funding acquisition. **Paulo Brito:** Supervision, Resources, Funding acquisition, Conceptualization. **Margarida Gonçalves:** Supervision, Resources, Methodology, Conceptualization. **Catarina Nobre:** Writing – review & editing, Visualization, Validation.

Declaration of competing interest

The authors declare that they have no known competing financial interests or personal relationships that could have appeared to influence the work reported in this paper.

References

[1] V. Forti, C.P. Balde, R. Kuehr, G. Bel, The Global E-Waste Monitor 2020: Quantities, Flows and the Circular Economy Potential, vol. 3, United Nations Univ (UNU)/United Nations Inst Train Res - Co-Hosted SCYCLE Program Int Telecommun Union Int Solid Waste Assoc (ISWA), Bonn/Geneva/Amsterdam, 2020, pp. 1–120.

[2] K. Bhaskar, B. Kumar, Electronic waste management and sustainable development goals: is there a business case for linking the two? J Indian Bus Res 11 (2019) 120–137, https://doi.org/10.1108/JIBR-01-2018-0051.

[3] D.S. Khetriwal, P. Kraeuchi, R. Widmer, Producer responsibility for e-waste management: key issues for consideration - learning from the Swiss experience, J. Environ. Manag. 90 (2009) 153–165, https://doi.org/10.1016/j.jenvman.2007.08.019.

[4] R. Widmer, H. Oswald-Krapf, D. Sinha-Khetriwal, M. Schnellmann, H. Böni, Global perspectives on e-waste, Environ. Impact Assess. Rev. 25 (2005) 436–458, https://doi.org/10.1016/j.eiar.2005.04.001.

[5] D.N. Perkins, M.N. Brune Drisse, T. Nxele, P.D. Sly, E-waste: a global hazard, Ann Glob Heal 80 (2014) 286–295, https://doi.org/10.1016/j.aogh.2014.10.001.

[6] V. Forti, C.P. Baldé, R. Kuehr. E-waste Statistics: Guidelines on Classifications, Reporting and Indicators, second edition, United Nations University, ViE – SCYCLE, Bonn, Germany, 2018.

[7] I.M.S.K. Ilankoon, Y. Ghorbani, M. Nan, G. Herath, T. Moyo, E-waste in the international context – a review of trade flows , regulations , hazards , waste management strategies and technologies for value recovery, Waste Manag. 82 (2018) 258–275, https://doi.org/10.1016/j.wasman.2018.10.018.

[8] Parlamento Europeu, Resíduos de equipamentos elétricos e eletrónicos na UE: factos e números (infografia), Europarl, 2023.

[9] X. Zeng, S.H. Ali, J. Tian, J. Li, Mapping anthropogenic mineral generation in China and its implications for a circular economy, Nat. Commun. 11 (2020) 1–9, https://doi.org/10.1038/s41467-020-15246-4.

[10] X. Wu, J. Li, L. Yao, Z. Xu, Auto-sorting commonly recovered plastics from waste household appliances and electronics using near-infrared spectroscopy, J. Clean. Prod. 246 (2020) 118732, https://doi.org/10.1016/j.jclepro.2019.118732.

[11] G. Martinho, A. Pires, L. Saraiva, R. Ribeiro, Composition of plastics from waste electrical and electronic equipment (WEEE) by direct sampling, Waste Manag. 32 (2012) 1213–1217, https://doi.org/10.1016/j.wasman.2012.02.010.

[12] J. Lee, A.K. Sarmah, E.E. Kwon, Production and formation of biochar, Biochar from Biomass Waste Fundam Appl (2018) 3–18, https://doi.org/10.1016/B978-0-12-811729-3.00001-7.

[13] W.J. Liu, H. Jiang, H.Q. Yu, Development of biochar-based functional materials: toward a sustainable platform carbon material, Chem. Rev. 115 (2015) 12251–12285, https://doi.org/10.1021/acs.chemrev.5b00195.

[14] H.S. Kambo, A. Dutta, A comparative review of biochar and hydrochar in terms of production, physico-chemical properties and applications, Renew. Sustain. Energy Rev. 45 (2015) 359–378, https://doi.org/10.1016/j.rser.2015.01.050.

[15] I. Queralt, J.M. Chimenos, J. Formosa, A. Maldonado-Alameda, S. Pérez-Martínez, J. Giro-Paloma, Characterisation and partition of valuable metals from WEEE in weathered municipal solid waste incineration bottom ash, with a view to recovering, J. Clean. Prod. 218 (2019) 61–68, https://doi.org/10.1016/j.jclepro.2019.01.313.

[16] M.P. Luda, Pyrolysis of WEEE plastics, Waste Electr Electron Equip Handb (2012) 239–263, https://doi.org/10.1533/9780857096333.2.239.

[17] X. Yang, L. Sun, J. Xiang, S. Hu, S. Su, Pyrolysis and dehalogenation of plastics from waste electrical and electronic equipment (WEEE): a review, Waste Manag. 33 (2013) 462–473, https://doi.org/10.1016/j.wasman.2012.07.025.

[18] B. Ebin, M.I. Isik, Chapter 5 - Pyrometallurgical Processes for the Recovery of Metals from WEEE, WEEE Recycl, 2016, pp. 107–137, https://doi.org/10.1016/B978-0-12-803363-0.00005-5.

[19] R.M. Panizio, L.F.C. Calado, O. Alves, C. Nobre, J.L. Silveira, P. Brito, et al., Effect of the Incorporation of Biomass in the Carbonization of Waste Electrical and Electronic Equipment, Bioenergy Conf., 2019.

[20] A. Gurgul, W. Szczepaniak, M. Zabłocka-Malicka, Incineration and pyrolysis vs. steam gasification of electronic waste, Psychol. Bull. 624 (2018) 1119–1124. .1037//0033-2909.I26.1.78.

[21] T. Furusawa, A. Tsutsumi, Comparison of Co/MgO and Ni/MgO catalysts for the steam reforming of naphthalene as a model compound of tar derived from biomass gasification, Appl. Catal. Gen. 278 (2005) 207–212, https://doi.org/10.1016/j.apcata.2004.09.035.

[22] Ö. Tezer, N. Karabağ, A. Öngen, C.Ö. Çolpan, A. Ayol, Biomass gasification for sustainable energy production: a review, Int. J. Hydrogen Energy 47 (2022) 15419–15433, https://doi.org/10.1016/j.ijhydene.2022.02.158.

[23] S. Mishra, R.K. Upadhyay, Review on biomass gasification: gasifiers, gasifying mediums, and operational parameters, Mater Sci Energy Technol 4 (2021) 329–340, https://doi.org/10.1016/j.mset.2021.08.009.

[24] R. Mishra, E. Singh, A. Kumar, A. Ghosh, S.-L. Lo, S. Kumar, Co-gasification of solid waste and its impact on final product yields, J. Clean. Prod. 374 (2022) 133989, https://doi.org/10.1016/j.jclepro.2022.133989.

[25] C. Ma, J. Yu, B. Wang, Z. Song, J. Xiang, S. Hu, et al., Chemical recycling of brominated flame retarded plastics from e-waste for clean fuels production: a review, Renew. Sustain. Energy Rev. 61 (2016) 433–450, https://doi.org/10.1016/j.rser.2016.04.020.

[26] K. Li, Z. Xu, A review of current progress of supercritical fluid technologies for e-waste treatment, J. Clean. Prod. 227 (2019) 794–809, https://doi.org/10.1016/j.jclepro.2019.04.104.

[27] P. Das, J.C.P. Gabriel, C.Y. Tay, J.M. Lee, Value-added products from thermochemical treatments of contaminated e-waste plastics, Chemosphere 269 (2021) 129409, https://doi.org/10.1016/j.chemosphere.2020.129409.

[28] S. Zhang, Y. Yu, Dechlorination behavior on the recovery of useful Resources from WEEE by the steam gasification in the molten carbonates, Procedia Environ Sci 31 (2016) 903–910, https://doi.org/10.1016/j.proenv.2016.02.108.

[29] T. Yamawaki, The gasification recycling technology of plastics WEEE containing brominated flame retardants, Plast Waste Manag Inst 27 (2003) 315–319, https://doi.org/10.1002/fam.833.

[30] J.C. Acomb, M.A. Nahil, P.T. Williams, Thermal processing of plastics from waste electrical and electronic equipment for hydrogen production, J. Anal. Appl. Pyrolysis 103 (2013) 320–327, https://doi.org/10.1016/j.jaap.2012.09.014.

[31] A. Anniwaer, N. Chaihad, A.C.A. Zahra, T. Yu, Y. Kasai, S. Kongparakul, et al., Steam co-gasification of Japanese cedarwood and its commercial biochar for hydrogen-rich gas production, Int. J. Hydrogen Energy 46 (2021) 34587–34598, https://doi.org/10.1016/j.ijhydene.2021.08.032.

[32] H. Tian, Y. Wei, S. Cheng, Z. Huang, M. Qing, Y. Chen, et al., Optimizing the gasification reactivity of biochar: the composition, structure and kinetics of biochar derived from biomass lignocellulosic components and their interactions during gasification process, Fuel 324 (2022) 124709, https://doi.org/10.1016/j.fuel.2022.124709.

[33] M. Zhai, Y. Zhang, P. Dong, P. Liu, Characteristics of rice husk char gasification with steam, Fuel 158 (2015) 42–49, https://doi.org/10.1016/j.fuel.2015.05.019.

[34] C. Muhammad, J.A. Onwudili, P.T. Williams, Catalytic pyrolysis of waste plastic from electrical and electronic equipment, J. Anal. Appl. Pyrolysis 113 (2015) 332–339, https://doi.org/10.1016/j.jaap.2015.02.016.

[35] E.V. Antonakou, K.G. Kalogiannis, S.D. Stephanidis, K.S. Triantafyllidis, A.A. Lappas, D.S. Achilias, Pyrolysis and catalytic pyrolysis as a recycling method of waste CDs originating from polycarbonate and HIPS, Waste Manag. 34 (2014) 2487–2493, https://doi.org/10.1016/j.wasman.2014.08.014.

[36] B.M. Caballero, I. de Marco, A. Adrados, A. López-Urionabarrenechea, J. Solar, N. Gastelu, Possibilities and limits of pyrolysis for recycling plastic rich waste streams rejected from phones recycling plants, Waste Manag. 57 (2016) 226–234, https://doi.org/10.1016/j.wasman.2016.01.002.

[37] C. Ma, J. Yu, B. Wang, Z. Song, F. Zhou, J. Xiang, et al., Influence of zeolites and mesoporous catalysts on catalytic pyrolysis of brominated acrylonitrile-butadiene-styrene (Br-abs), Energy Fuel. 30 (2016) 4635–4643, https://doi.org/10.1021/acs.energyfuels.6b00460.

[38] T. Bhaskar, K. Murai, T. Matsui, M.A. Brebu, M.A. Uddin, A. Muto, et al., Studies on thermal degradation of acrylonitrile-butadiene-styrene copolymer (ABS-Br) containing brominated flame retardant, J. Anal. Appl. Pyrolysis 70 (2003) 369–381, https://doi.org/10.1016/S0165-2370(02)00183-3.

[39] Y.B. Zhao, X.D. Lv, H.G. Ni, Solvent-based separation and recycling of waste plastics: a review, Chemosphere 209 (2018) 707–720, https://doi.org/10.1016/j.chemosphere.2018.06.095.

[40] W.J. Hall, P.T. Williams, Removal of organobromine compounds from the pyrolysis oils of flame retarded plastics using zeolite catalysts, J. Anal. Appl. Pyrolysis 81 (2008) 139–147, https://doi.org/10.1016/j.jaap.2007.09.008.

[41] E.C. Vouvoudi, A.T. Rousi, D.S. Achilias, Thermal degradation characteristics and products obtained after pyrolysis of specific polymers found in Waste Electrical and Electronic Equipment, Front. Environ. Sci. Eng. 11 (2017), https://doi.org/10.1007/s11783-017-0996-5.

[42] S.D. Anuar Sharuddin, F. Abnisa, W.M.A. Wan Daud, M.K. Aroua, A review on pyrolysis of plastic wastes, Energy Convers. Manag. 115 (2016) 308–326, https://doi.org/10.1016/j.enconman.2016.02.037.

[43] A. Marino, A. Aloise, H. Hernando, J. Fermoso, D. Cozza, E. Giglio, et al., ZSM-5 zeolites performance assessment in catalytic pyrolysis of PVC-containing real WEEE plastic wastes, Catal. Today 390–391 (2022) 210–220, https://doi.org/10.1016/j.cattod.2021.11.033.

[44] Y. Wang, R. Yoshiie, Y. Ueki, I. Naruse, Effect of temperature on behavior and mechanism of biochar gasification in the mixed CO2 and H2O atmosphere, J. Energy Inst. 108 (2023) 101238, https://doi.org/10.1016/j.joei.2023.101238.

[45] A. Skreiberg, O. Skreiberg, J. Sandquist, L. Sørum, TGA and macro-TGA characterisation of biomass fuels and fuel mixtures, Fuel 90 (2011) 2182–2197, https://doi.org/10.1016/j.fuel.2011.02.012.

[46] A. Fernandez, J. Soria, R. Rodriguez, J. Baeyens, G. Mazza, Macro-TGA steam-assisted gasification of lignocellulosic wastes, J. Environ. Manag. 233 (2019) 626–635, https://doi.org/10.1016/j.jenvman.2018.12.087.

[47] H. Zhou, Y. Long, A. Meng, S. Chen, Q. Li, Y. Zhang, A novel method for kinetics analysis of pyrolysis of hemicellulose, cellulose and lignin in TGA and macro-TGA, RSC Adv. 5 (2015) 26509–26516, https://doi.org/10.1039/C5RA02715B.

[48] A. Meng, S. Chen, Y. Long, H. Zhou, Y. Zhang, Q. Li, Pyrolysis and gasification of typical components in wastes with macro-TGA, Waste Manag. 46 (2015) 247–256, https://doi.org/10.1016/j.wasman.2015.08.025.

[49] Y. Long, A. Meng, S. Chen, H. Zhou, Y. Zhang, Q. Li, Pyrolysis and combustion of typical wastes in a newly designed macro thermogravimetric analyzer: characteristics and simulation by model components, Energy Fuel. 31 (2017) 7582–7590, https://doi.org/10.1021/acs.energyfuels.7b00796.

[50] R. Mota-Panizio, M.J. Hermoso-Orzáez, L. Carmo-Calado, H. Calado, M.M. Goncalves, P. Brito, Co-carbonization of a mixture of waste insulation electric cables (WIEC) and lignocellulosic waste, for the removal of chlorine: biochar properties and their behaviors, Fuel 320 (2022), https://doi.org/10.1016/j.fuel.2022.123932.

[51] C. Nobre, C. Vilarinho, O. Alves, B. Mendes, M. Gonçalves, Upgrading of refuse derived fuel through torrefaction and carbonization: evaluation of RDF char fuel properties, Energy 181 (2019), https://doi.org/10.1016/j.energy.2019.05.105.

[52] Z. Liu, The Fate of Fluorine and Chlorine during Thermal Treatment of Coals, vol. 40, 2006, pp. 7886–7889.

[53] A. Longo, C. Nobre, A. Sen, R. Panizio, P. Brito, M. Gonçalves, Torrefaction upgrading of heterogenous wastes containing cork and chlorinated polymers, Environments 99 (2022) 1–21.

[54] R. Mota-Panizio, L. Carmo-Calado, A.C. Assis, V. Matos, M.J. Hermoso-Orzáez, P. Romano, M. Gonçalves, P. Brito, Properties and Uses of Biochars Incorporated into Mortars, Environments 10 (2023) 47.

[55] Y. Wei, M. Chen, S. Niu, X. You, F. Xue, Evaluation on oxy-fuel co-combustion behavior of Chinese lignite and eucalyptus bark, J. Therm. Anal. Calorim. 123 (2016) 1667–1684, https://doi.org/10.1007/s10973-015-5050-x.

[56] S. Zhang, T. Chen, W. Li, Q. Dong, Y. Xiong, Physicochemical properties and combustion behavior of duckweed during wet torrefaction, Bioresour. Technol. 218 (2016) 1157–1162, https://doi.org/10.1016/j.biortech.2016.07.086.

[57] L.G. Fraga, J. Silva, S. Teixeira, D. Soares, M. Ferreira, J. Teixeira, Influence of Operating Conditions on the Thermal Behavior and Kinetics of Pine Wood Particles Using Thermogravimetric Analysis, 2020, pp. 1–22.

[58] S. Park, C. Jang, Characteristics of carbonized sludge for co-combustion in pulverized coal power plants, Waste Manag. 31 (2011) 523–529, https://doi.org/10.1016/j.wasman.2010.10.009.

[59] A. Atımtay, F.D. Sanin, Comparison of Fuel Value and Combustion Characteristics of Two Different RDF Samples, vol. 47, 2016, pp. 217–224, https://doi.org/10.1016/j.wasman.2015.08.037.

[60] Y. Furusawa, H. Taguchi, S.N. Ismail, S. Thangavel, K. Matsuoka, C. Fushimi, Estimation of cold gas efficiency and reactor size of low-temperature gasifier for advanced-integrated coal gasification combined cycle systems, Fuel Process. Technol. 193 (2019) 304–316, https://doi.org/10.1016/j.fuproc.2019.05.023.

[61] M.K. Cohce, I. Dincer, M.A. Rosen, Thermodynamic analysis of hydrogen production from biomass gasification, Int. J. Hydrogen Energy 35 (2010) 4970–4980, https://doi.org/10.1016/j.ijhydene.2009.08.066.

[62] J. Josâ, Kinetics of Devolatilisation of Forestry Wastes from Thermogravimetric Analysis, vol. 27, 2004, pp. 385–391, https://doi.org/10.1016/j.biombioe.2003.11.010.

[63] James A. Ippolito, Kurt A. Spokas, Jeffrey M. Novak Rdl, KBC. Biochar elemental composition and factors influencing nutrient retention, in: J.L. Joseph, S (Eds.), Biochar Environ. Manag. Sci. Technol. Implement., 2015.

[64] R. Sun, T.M. Ismail, X. Ren, M. Abd El-Salam, Effect of ash content on the combustion process of simulated MSW in the fixed bed, Waste Manag. 48 (2016) 236–249, https://doi.org/10.1016/j.wasman.2015.10.007.

[65] R. Correia, M. Gonçalves, C. Nobre, B. Mendes, Impact of torrefaction and low-temperature carbonization on the properties of biomass wastes from Arundo donax L. and Phoenix canariensis, Bioresour. Technol. 223 (2017), https://doi.org/10.1016/j.biortech.2016.10.046.

[66] H. Knicker, Stabilization of N-compounds in soil and organic-matter-rich sediments - what is the difference? Mar. Chem. 92 (2004) 167–195, https://doi.org/10.1016/j.marchem.2004.06.025.

[67] A. Anand, S. Gautam, L.C. Ram, Feedstock and pyrolysis conditions affect suitability of biochar for various sustainable energy and environmental applications, J. Anal. Appl. Pyrolysis 170 (2023) 105881, https://doi.org/10.1016/j.jaap.2023.105881.

[68] M.D. Bispo, J.K. Schneider, D. Da Silva Oliveira, D. Tomasini, G.P. Da Silva MacIel, T. Schena, et al., Production of activated biochar from coconut fiber for the removal of organic compounds from phenolic, J. Environ. Chem. Eng. 6 (2018) 2743–2750, https://doi.org/10.1016/j.jece.2018.04.029.

[69] D. Ma, S. Jia, Z. Hu, X. Wang, L. Li, H. Tan, Experimental investigation of water washing effect on high-chlorine coal properties, Fuel 319 (2022) 123838, https://doi.org/10.1016/j.fuel.2022.123838.

[70] S.K. Hoekman, A. Broch, C. Robbins, Hydrothermal carbonization (HTC) of lignocellulosic biomass, Energy Fuel. 25 (2011) 1802–1810, https://doi.org/10.1021/ef101745n.

[71] W. Yang, H. Wang, M. Zhang, J. Zhu, J. Zhou, S. Wu, Fuel properties and combustion kinetics of hydrochar prepared by hydrothermal carbonization of bamboo, Bioresour. Technol. 205 (2016) 199–204, https://doi.org/10.1016/j.biortech.2016.01.068.

[72] S. Kim, P. Omur-Ozbek, K. Carlson, Characterization of organic matter in water from oil and gas wells hydraulically fractured with recycled water, J. Hazard Mater. 397 (2020) 120551, https://doi.org/10.1016/j.jhazmat.2019.04.034.

[73] U.M. Ikegwu, N.M. Okoro, M. Ozonoh, M.O. Daramola, Thermogravimetric properties and degradation kinetics of biomass during its thermochemical conversion process, Mater Today Proc (2022), https://doi.org/10.1016/j.matpr.2022.05.538.

[74] J. Cai, Y. He, X. Yu, S.W. Banks, Y. Yang, X. Zhang, et al., Review of physicochemical properties and analytical characterization of lignocellulosic biomass, Renew. Sustain. Energy Rev. 76 (2017) 309–322, https://doi.org/10.1016/j.rser.2017.03.072.

[75] Y. Niu, H. Tan, L. Ma, M. Pourkashanian, Z. Liu, Y. Liu, et al., Slagging Characteristics on the Superheaters of a 12 MW Biomass-Fired Boiler, vol. 79, 2010, pp. 5222–5227, https://doi.org/10.1021/ef1008055.
[76] D. Vamvuka, M. Trikouvertis, D. Pentari, G. Alevizos, A. Stratakis, Characterization and evaluation of fl y and bottom ashes from combustion of residues from vineyards and processing industry, J. Energy Inst. 90 (2017) 574–587, https://doi.org/10.1016/j.joei.2016.05.004.
[77] X. Lin, Y. Yang, S. Yang, S. Li, Y. Tian, Y. Wang, Initial deposition feature during high-temperature pressurized pyrolysis of a typical zhundong coal. https://doi.org/10.1021/acs.energyfuels.6b01074, 2016.
[78] C. Wang, R. Sun, C. Liu, T. Han, C. Zhu, Y. Liu, et al., Experimental study on morphology and chemical composition of ash deposition during oxy-fuel combustion of high-alkali coal. https://doi.org/10.1021/acs.energyfuels.9b00028, 2019.
[79] D. Nutalapati, R. Gupta, B. Moghtaderi, T.F. Wall, Assessing Slagging and Fouling during Biomass Combustion : A Thermodynamic Approach Allowing for Alkali/Ash Reactions, vol. 88, 2007, pp. 1044–1052, https://doi.org/10.1016/j.fuproc.2007.06.022.
[80] H. Se, H. Wiinikka, B. Lindblom, L.O. Nordin, G. Wu, E. Yazhenskikh, Comparison of High-Rank Coals with Respect to Slagging/deposition Tendency at the Transfer-Chute of Iron-Ore Pelletizing Grate-Kiln Plants: A Pilot-Scale Experimental Study Accompanied by Thermochemical Equilibrium Modeling and Viscosity Estimations, vol. 193, 2019, pp. 244–262, https://doi.org/10.1016/j.fuproc.2019.05.026.
[81] T.Y. Jeong, L. Sh, J.H. Kim, B.H. Lee, C.H. Jeon, Experimental investigation of ash deposit behavior during co-combustion of bituminous coal with wood pellets and empty fruit bunches, Energies 12 (2019), https://doi.org/10.3390/en12112087.
[82] J.B. Kitto, S.C. Stultz, Steam: its Generation and Use, Babcock Wilcox Co, 2005.
[83] J.E.C. Garcı, Comparing Methods for Predicting the Sintering of Biomass Ash in Combustion, vol. 84, 2005, pp. 1893–1900, https://doi.org/10.1016/j.fuel.2005.04.010.
[84] C. Serrano, H. Portero, E. Monedero, Pine chips combustion in a 50 kW domestic biomass boiler, Fuel 111 (2013) 564–573, https://doi.org/10.1016/j.fuel.2013.02.068.
[85] C. Nobre, O. Alves, L. Durão, A. Şen, C. Vilarinho, M. Gonçalves, Characterization of hydrochar and process water from the hydrothermal carbonization of Refuse Derived Fuel, Waste Manag. 120 (2021), https://doi.org/10.1016/j.wasman.2020.11.040.
[86] G. Wang, J. Zhang, J. Shao, Z. Liu, G. Zhang, T. Xu, et al., Thermal behavior and kinetic analysis of co-combustion of waste biomass/low rank coal blends, Energy Convers. Manag. 124 (2016) 414–426, https://doi.org/10.1016/j.enconman.2016.07.045.
[87] K. Cong, F. Han, Y. Zhang, Q. Li, The investigation of co-combustion characteristics of tobacco stalk and low rank coal using a macro-TGA, Fuel 237 (2019) 126–132, https://doi.org/10.1016/j.fuel.2018.09.149.
[88] S. Wu, Z. Li, Experimental and modeling study on centimeter pine char combustion in fast-heating Macro TGA, Proc. Combust. Inst. 39 (2023) 3497–3508, https://doi.org/10.1016/j.proci.2022.08.080.
[89] J. Natarajan, T. Lieuwen, J. Seitzman, Laminar Flame Speeds of H2/CO Mixtures: Effect of CO2 Dilution, Preheat Temperature, and Pressure, vol. 151, 2007, pp. 104–119, https://doi.org/10.1016/j.combustflame.2007.05.003.
[90] M.S.M. Said, W.A.W.A.K. Ghani, H.B. Tan, D.K.S. Ng, Prediction and optimisation of syngas production from air gasification of Napier grass via stoichiometric equilibrium model, Energy Convers. Manag. X 10 (2021) 100057, https://doi.org/10.1016/j.ecmx.2020.100057.
[91] F. Weiland, H. Wiinikka, H. Hedman, J. Wennebro, E. Pettersson, R. Gebart, Influence of process parameters on the performance of an oxygen blown entrained flow biomass gasifier, Fuel 153 (2015) 510–519, https://doi.org/10.1016/j.fuel.2015.03.041.
[92] W. Lu, Q. Cao, B. Xu, H. Adidharma, K. Gasem, M. Argyle, et al., A new approach of reduction of carbon dioxide emission and optimal use of carbon and hydrogen content for the desired syngas production from coal, J. Clean. Prod. 265 (2020) 121786, https://doi.org/10.1016/j.jclepro.2020.121786.
[93] A. Lampropoulos, V. Binas, M. Konsolakis, G.E. Marnellos, Steam gasification of Greek lignite and its chars by co-feeding CO2 toward syngas production with an adjustable H2/CO ratio, Int. J. Hydrogen Energy 46 (2021) 28486–28500, https://doi.org/10.1016/j.ijhydene.2021.06.131.
[94] A. Anca-Couce, P. Sommersacher, A. Shiehnejadhesar, R. Mehrabian, C. Hochenauer, R. Scharler, CO/CO2 ratio in biomass char oxidation, Energy Proc. 120 (2017) 238–245, https://doi.org/10.1016/j.egypro.2017.07.170.
[95] F. Scala, A new technique for the measurement of the product CO/CO2 ratio at the surface of char particles burning in a fluidized bed, Proc. Combust. Inst. 32 (II) (2009) 2021–2027, https://doi.org/10.1016/j.proci.2008.06.047.
[96] Y. Li, K. Luo, Y. Tang, G. Lin, G. Lu, F. Gong, Progesterone/estradiol ratio < 0.25 on the day of human chorionic gonadotropin administration is associated with adverse pregnancy outcomes in prolonged protocols for in vitro fertilization/intracytoplasmic sperm injection, Taiwan. J. Obstet. Gynecol. 56 (2017) 27–31, https://doi.org/10.1016/j.tjog.2016.05.013.